

Supplementary materials

Target-triggered cascade recycling amplification for label-free detection of microRNA and molecular logic operations

Sai Bi^{a*}, Jiayan Ye^b, Ying Dong^b, Haoting Li^a and Wei Cao^b

^a*Collaborative Innovation Center for Marine Biomass Fiber Materials and Textiles, College of Chemical Science and Engineering, Laboratory of Fiber Materials and Modern Textiles, the Growing Base for State Key Laboratory, Shandong Sino-Japanese Center for Collaborative Research of Carbon Nanomaterials, Qingdao University, Qingdao 266071, P.R.China.*

^b*Key Laboratory of Sensor Analysis of Tumor Marker, Ministry of Education, College of Chemistry and Molecular Engineering, Qingdao University of Science and Technology, Qingdao 266042, P.R.China*

*Corresponding author. E-mail address: bisai11@126.com.

1. Materials and methods

1.1. Reagents and apparatus

The oligonucleotides were synthesized and HPLC purified by Takara Biotechnology Co., Ltd. (Dalian, China), and the sequences are listed in [Table S1](#). The DNAs that were used to attach on carboxyl-MNPs are modified with amino groups at 5'-end for OR, AND and INHIBIT gates, while at 3'-end for NOR, NAND and IMPICATION gates. The domain sequences are presented in [Table S2](#). The Klenow fragment exo- DNA polymerase and Nt.BbvCI nicking endonuclease were purchased from Fermentas (Canada) and New England Biolabs Inc. (USA), respectively. The deoxyribonucleoside triphosphates (dNTPs) mix was obtained from SBS Genetech Co., Ltd. (Beijing, China). Hemin, luminol, 2-[4-(2-hydroxyethyl)-1-piperazinyl]ethanesulfonic acid (HEPES) were purchased from Aladdin Chemistry Co. Ltd (China). Carboxyl-modified MNPs (100~200 nm) and magnetic rack were custom-ordered from BaseLine Chromtech Research Centre (Tianjin, China). All reagents were of analytical grade, which were used as received unless otherwise stated. Double-distilled deionized water was used throughout the experiments. The CL measurements were performed on a Centro LB942 luminometer (Berthold, Germany).

1.2. Target-triggered CRA for CL detection of miR-122

Firstly, HP1 and HP2 were respectively annealed by heating at 95 °C for 5 min, gradually cooling 1 °C/min to 20 °C, and standing at 20 °C for 1 h at least to obtain desirable secondary structures. The CRA reaction was performed by mixing 10 µL of HP1 (1 µM) and 10 µL of HP2 (1 µM) with 10 µL of miR-122 at different concentrations, followed by addition of 15 µL solution containing Klenow fragment exo- polymerase (10 U), Nt.BbvCI nicking endonuclease (10 U), 1× NEBuffer2 (50 mM NaCl, 10 mM Tris-HCl, 10 mM MgCl₂, 1 mM DTT, pH 7.9), 1× CutSmart® Buffer (50

mM KAc, 20 mM Tris-HAc, 10 mM MgAc₂, 100 µg/mL BSA, pH 7.9), and dNTPs (10 mM), and then incubated at 37 °C for 2 h. The resulting products were reacted with 10 µL of hemin (1 µM) in HEPES buffer (25 mM, pH 7.4) consisting of 20 mM KCl, 200 mM NaCl, 1% DMSO (v/v), 0.05% Triton C-100 (w/v) for 30 min at room temperature. The CL signals were measured by addition of 90 µL of luminol (50 µM) and 20 µL of H₂O₂ (5 mM).

The control experiments were carried out as the above procedures, except that no Nt.BbvCI nicking endonuclease and CutSmart® Buffer was added (Scheme S1), or no Klenow fragment exo- polymerase, Nt.BbvCI nicking endonuclease, NEBuffer2, CutSmart® Buffer and dNTPs was added (Scheme S2). It should be noted that the volume of each sample was supplemented to 45 µL by TE buffer.

1.3. Preparation of DNA-MNPs conjugates

Firstly, a 10 µL of carboxyl-modified MNPs (10 mg/ml) was washed with imidazole-HCl solution (0.1 M, pH 6.8) twice. Then, the carboxyl groups on MNPs were activated by 200 µL of EDC (0.1 M) and NHS (0.01 M) at room temperature for 30 min. After magnetic separation, 10 µL of corresponding amino-modified DNA (1 µM) was added, followed by incubation at 37 °C overnight. After rinsing with PBS solution (10 mM, pH 7.4) three times, the resulting DNA-MNP conjugates were re-suspended in PBS solution and stored at 4 °C until use.

1.4. Logic operations

For OR, AND, and INHIBIT gates, corresponding DNA-MNP conjugates were firstly mixed with 10 µL of miR-122 (100 pM), 10 µL of miR-let-7a (100 pM), and 10 µL of miR-122 (100 pM) and miR-let-7a (100 pM), respectively, and incubated at room temperature for 1 h. After magnetic separation, 10 µL of corresponding HP1 (1 µM) and 10 µL of corresponding HP2 (1 µM) were

added to the resulting supernatant. The following steps were carried out as mentioned in Section 1.2.

For NOR, NAND, and IMPLICATION gates, corresponding DNA-MNP conjugates were firstly mixed with 10 μ L of miR-122 (100 pM), 10 μ L of miR-let-7a (100 pM), and 10 μ L of miR-122 (100 pM) and miR-let-7a (100 pM), respectively, and incubated at room temperature for 1 h. After magnetic separation, 10 μ L of corresponding additional DNA (200 pM) was added to the resulting supernatant and incubated at room temperature for another 1 h, followed by addition of 10 μ L of corresponding HP1 (1 μ M) and 10 μ L of corresponding HP2 (1 μ M). The following steps were carried out as mentioned in Section 1.2.

Table S1. Sequences of oligonucleotides used for miR-122 detection

name	Sequences (from 5' to 3')
miR-122	UGGAGUGUGACAAUGGUGUUUG
miR-let-7a	UGAGGUAGUAGGUUGUAUAGUU
miR-let-7b	UGAGGUAGUAGGUUGUGUGGUU
miR-let-7c	UGAGGUAGUAGGUUGUAUGGUU
HP1	CAAACACCATTGTCACACTCCACCTCAGCGGTGTTTGCCCAACCCGCC
HP2	CCCAACCCGCCCTACCCCTCAGCGGCGGGTTGGGCAAACACC
HP1''	CAAACACCATTGTCACACTCCAGGTGTTTGGGGTAGGGCGG
HP2'	GGGTAGGGCGGGTTGGGCCGCCCTACCCCAAACACC
HP1'	CAAACACCATTGTCACACTCCAGGTGTTTGGGGTAGGGCGGTTTTTT
HP1-I	GCCATAGCATCGCTACCTAACGCCTCAGCGCTATGGCCCAACCCGCC
HP2-I	CCCAACCCGCCCTACCCCTCAGCGGCGGGTTGGGGCCATAGC
HP1-II	ATTGTCACACTCCAAACTATAACCTCAGCGTGACAATCCCAACCCGCC
HP2-II	CCCAACCCGCCCTACCCCTCAGCGGCGGGTTGGGATTGTCAC
HP1-III	TGGAGTGTGACAATGGTGTTCCTCAGCACTCCACCCAACCCGCC
HP2-III	CCCAACCCGCCCTACCCCTCAGCGGCGGGTTGGGTGGAGT
HP1-IV	GTATAGTTTGGAGTGTGACAATCCTCAGCAACTATAACCCCAACCCGCC
HP2-IV	CCCAACCCGCCCTACCCCTCAGCGGCGGGTTGGGGTATAGTT
ADD	CAAACACCATTGTCACACTCCA
ADD-I	CGTTAGGTAGCGATGCTATGGC
ADD-II	ATTGTCACACTCCAAACTATAC
ADD-III	TGGAGTGTGACAATGGTGTTTG

Table S2. Sequences of oligonucleotide used for logic operation

name	Sequences (from 5' to 3')
a	CAAACACC
b	ATTGTCACACTCCA
b ₁	ATTGTCAC
b ₂	ACTCCA
c	CCCAACCCGCC
e	AACTATAC
f	AACCTACTACCTCA
f ₁	AACCTACT
f ₂	ACCTCA
g	GCTATGGC
h	CGTTAGGTAGCGAT
x	CCTCAGC

2. Non-denaturing polyacrylamide gel electrophoresis (PAGE) characterization

The yield ratio of every step is studied by non-denaturing polyacrylamide gel electrophoresis (PAGE). To make the results clear, target miR-122, HP1, and HP2 are at the same concentration of 1 μ M. For the YES-YES cascade gates that are operated via toehold-mediated strand displacement reaction to cascade open DNA hairpins (Fig. S1A), quantitation of the gel fragments shows approximately 100% yield for the products of HP1 (lane 1), target/HP1 complex (lane 2) and target/HP1/HP2 complex (lane 3). Moreover, for the cascade AND-AND recycling amplification (Fig. S1B), a DNA polymerization reaction is initiated in the presence of Klenow fragment exo- DNA polymerase/dNTPs, resulting in the formation of a long double-stranded DNA (dsDNA) and displacement of target miR-122 (lane 4). In comparison with the hybrid of target/HP1/HP2 (lane 3), the long dsDNA in lane 4 has more base pairs, so that it migrates a bit slower than target/HP1/HP2 complex. In addition, since the target miR-122 is too short with only 22 nucleotides (nt) and SYBR Green I stains single-stranded nucleic acid much less efficiently than double-stranded one, the displaced miR-122 is difficult to be observed in gel. Upon addition of Nb.BbvCI endonuclease, Cycle II in Scheme 1A of displacement, nicking and polymerization are activated, during which a large amount of trigger DNAs and HRP-mimicking DNAzyme sequences are synthesized (lane 5). Moreover, from the detection sensitivity assay, in comparison with the detection limit obtained by only Cycle I to amplify signal (0.17 pM, Scheme S1) and no amplification method (8.9 pM, Scheme S2), the detection sensitivity is improved to 0.82 fM, which also indicating the high yield of every step and high amplification efficiency of the CRA.

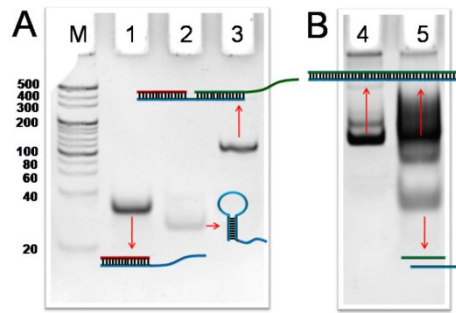


Fig. S1 Non-denaturing PAGE of the reaction pathways. (A) YES-YES cascade gates to open DNA hairpins and (B) cascade AND-AND recycling amplification to activate the feedback amplification function. Lane M: 500-bp marker; lane 1: HP1; lane 2: target miR-122 + HP1; lane 3: target miR-122 + HP1 + HP2; lane 4: target miR-122 + HP1 + HP2 + Klenow fragment exo-DNA polymerase/dNTPs; lane 5: target miR-122 + HP1 + HP2 + Klenow fragment exo-DNA polymerase/dNTPs + Nb.BbvCI endonuclease. The concentrations of miR-122, HP1, and HP2 are 1 μ M, respectively. The amounts of Klenow fragment exo- polymerase and Nt.BbvCI nicking endonuclease are 10 U, respectively.

3. Comparison of target recycling amplification strategies for miRNA detection

Table S3. Comparison of target recycling amplification strategies for miRNA detection

Amplification strategy	Detection technique	LOD	Ref.
Endonuclease-assisted target recycling amplification using Ag nanocluster as fluorophore	fluorescence	0.16 nM	¹
Enzyme-assisted strand cycle exponential signal amplification and DNA-bio-bar-code amplification	fluorescence	52.5 zM	²
Ligase chain reaction and Lambda exonuclease-assisted cationic conjugated polymer biosensing	fluorescence	0.1 fM	³
Duplex-specific nuclease-assisted nanoparticle amplification	colorimetric detection	16 pM	⁴
DNA molecular machine for non-enzymatic target recycling amplification	fluorescence	80 fM	⁵
Polymerase-aided strand displacement amplification and Lambda exonuclease-assisted cyclic enzymatic amplification	fluorescence	0.3 pM	⁶
Enzyme-free signal amplification of catalyzed hairpin assembly	fluorescence	1 pM	⁷
Cyclic enzyme amplification and resonance energy transfer	electrochemiluminescence	0.24 fM	⁸
Cyclic enzymatic amplification based on graphene oxide-protected DNA probes	fluorescence	9 pM	⁹
T7 exonuclease-assisted cyclic enzymatic amplification method coupled with rolling circle amplification	fluorescence	12 fM	¹⁰
Target-triggered cascade recycling amplification	chemiluminescence	0.82 fM	this assay

4. Specificity of the proposed CRA for miRNA analysis

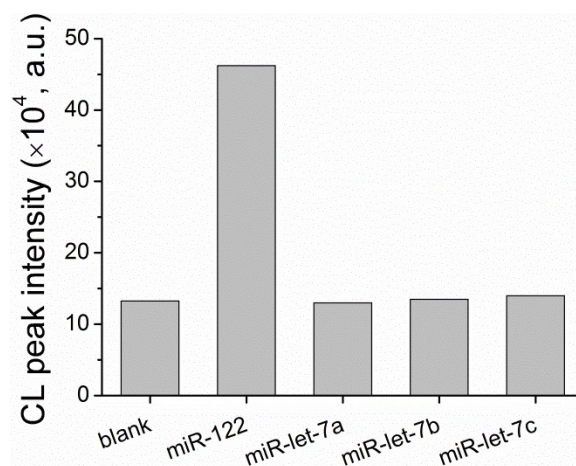
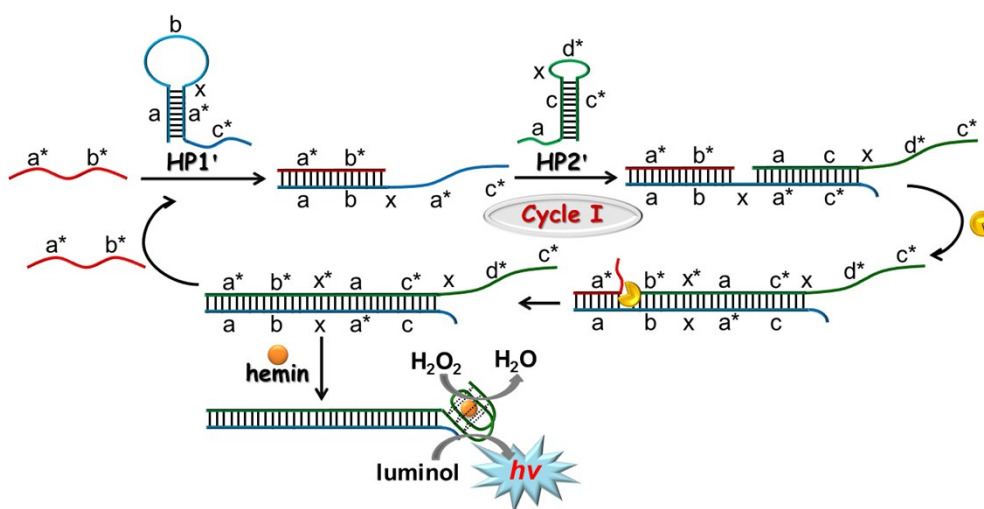


Fig. S2 CL peak intensity of the CRA triggered by different miRNAs. The concentration of each miRNA is 1 pM.

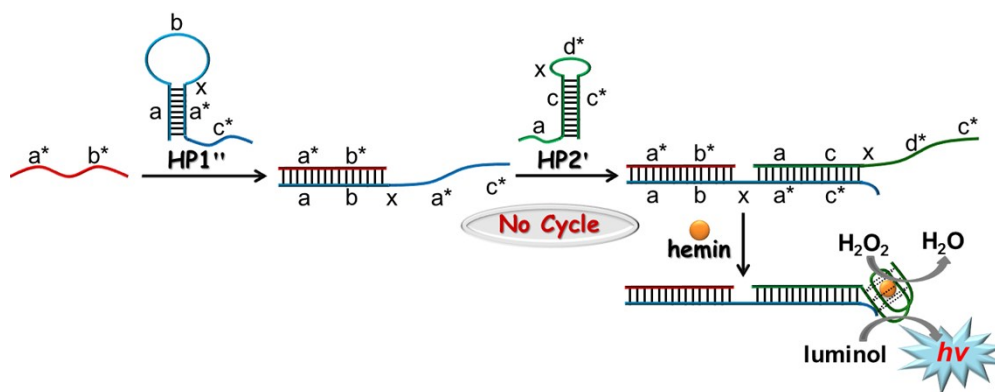
5. Control experiments

5.1. Control experiment-I



Scheme S1 Schematic illustration of the target-triggered recycling amplification of Cycle I for label-free CL analysis of miRNA.

5.2. Control experiment-II



Scheme S2 Schematic illustration of the target-triggered cascade opening of HP1 and HP2 for label-free CL analysis of miRNA without recycling amplification.

6. Logic operations

6.1. AND gate

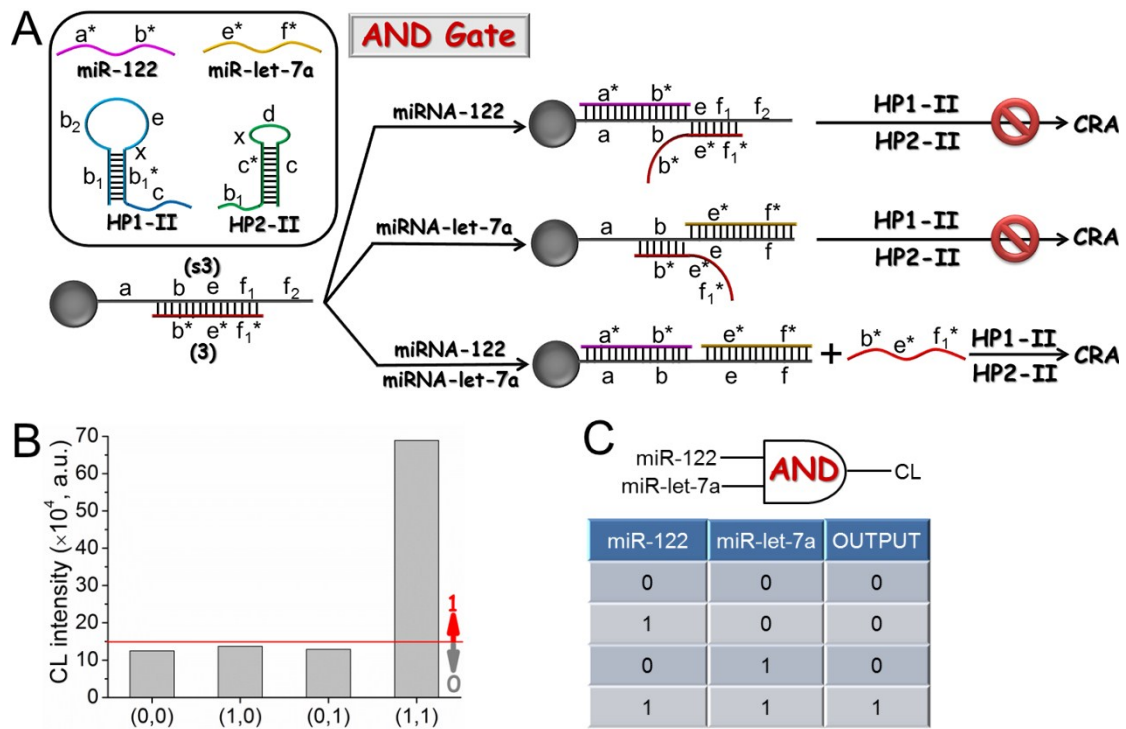


Fig. S3 (A) Diagrammatic representation, (B) CL results, and (C) truth table of AND logic gate that is activated by miR-122 and miR-let-7a as inputs and connected to CRA reaction to produce CL outputs.

6.2. INHIBIT gate

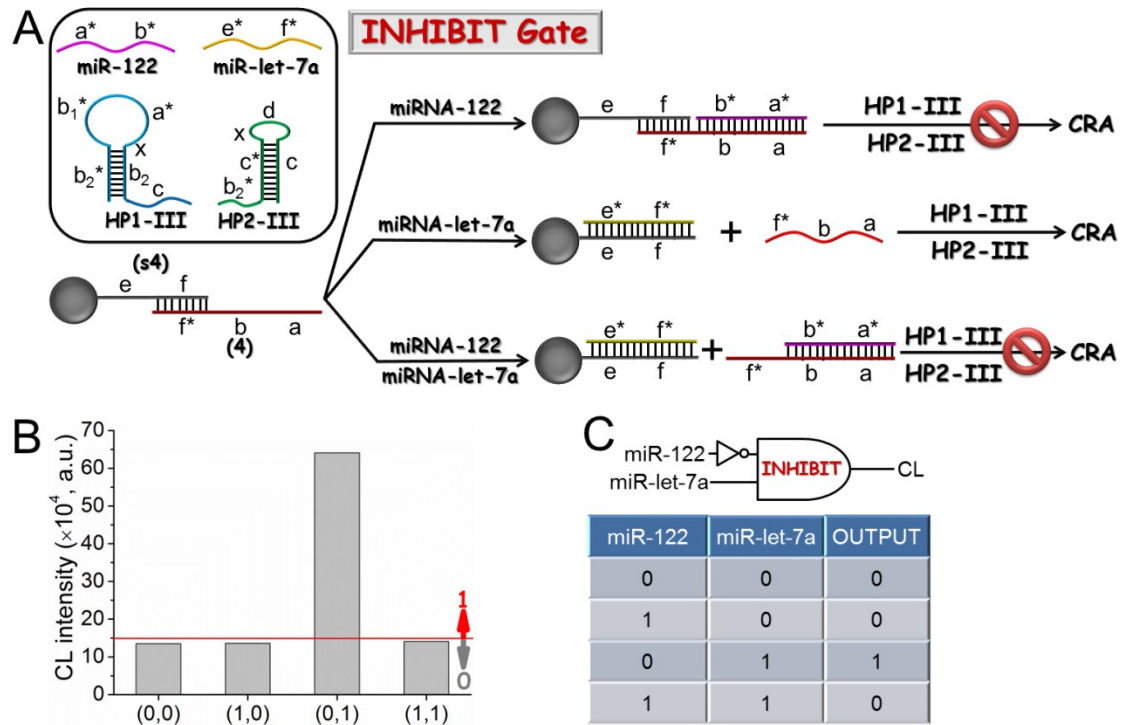


Fig. S4 (A) Diagrammatic representation, (B) CL results, and (C) truth table of INHIBIT logic gate that is activated by miR-122 and miR-let-7a as inputs and connected to CRA reaction to produce CL outputs.

6.3. NOR gate

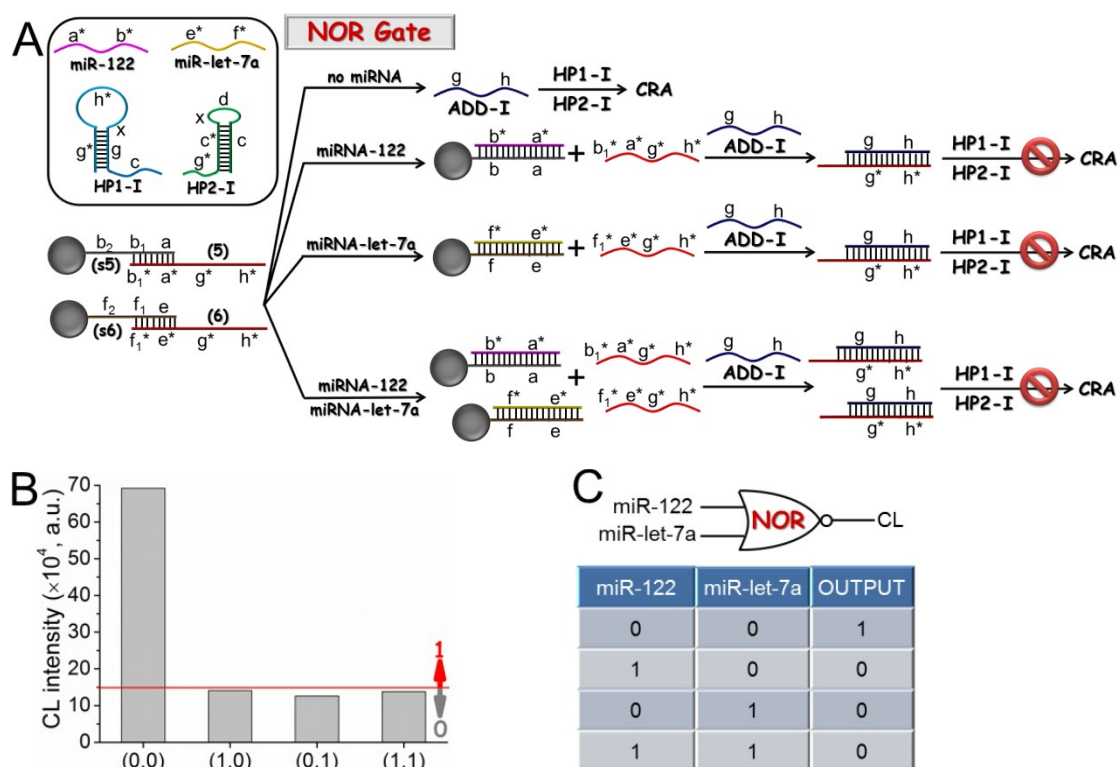


Fig. S5 (A) Diagrammatic representation, (B) CL results, and (C) truth table of NOR logic gate that is activated by miR-122 and miR-let-7a as inputs and connected to CRA reaction to produce CL outputs.

For a NOR gate (Scheme 3B), the overhang of DNA (5) or (6) (domain g^*h^*) is complementary to ADD-I. In the presence of either input miR-122 or miR-let-7a as well as both inputs, DNA (5) and DNA (6) pre-hybridized with the substrate is dissociated from MNPs and hybridized with the following added ADD-I after magnetic separation. As a result, the trigger of CRA is eliminated by hybridization between ADD-I and the released DNA (5) and (6), leading to the false output of the gate. The results of NOR can be considered as sending an OR gate through an inverter, which causes all 0 states to switch to 1 and vice versa. The reaction pathways, corresponding CL results and truth table of NOR gate are presented in Fig. S4.

6.4. NAND gate

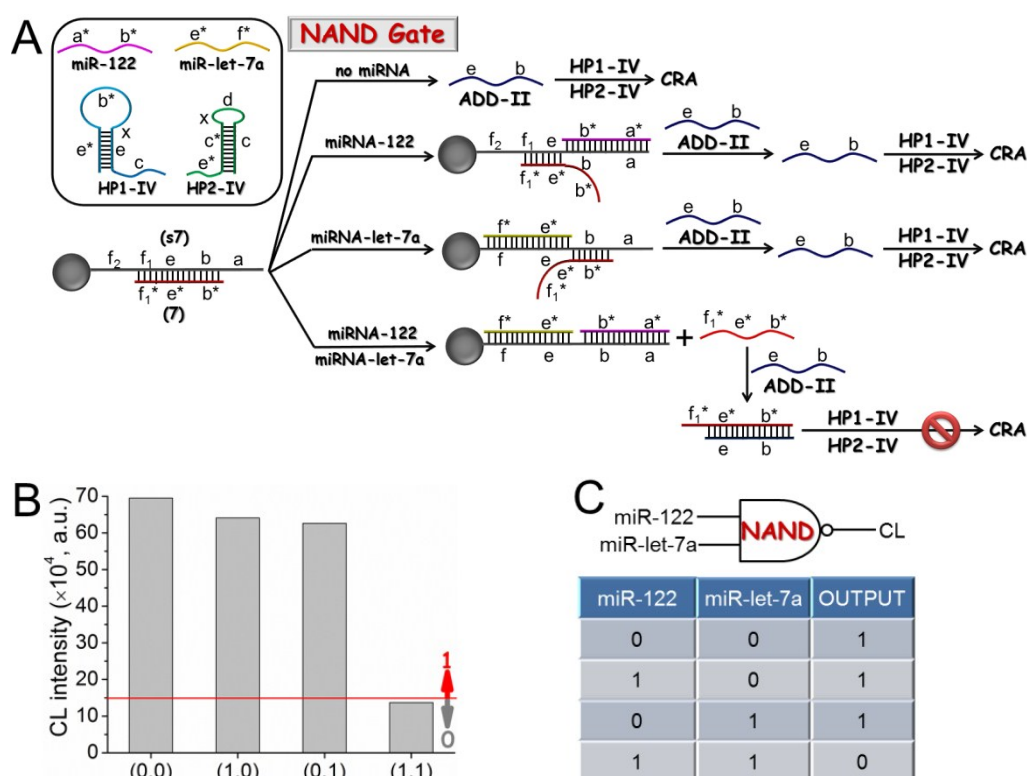


Fig. S6 (A) Diagrammatic representation, (B) CL results, and (C) truth table of NAND logic gate that is activated by miR-122 and miR-let-7a as inputs and connected to CRA reaction to produce CL outputs.

For a NAND gate (Scheme 3C), similar to AND gate, in the presence of either input miR-122 or miR-let-7a, DNA (7) cannot be displaced from the substrate (s7). Thus, after magnetic separation, ADD-II can act as a trigger to activate the CRA, leading to a true output. In contrast, the presence of both inputs, miR-122 and miR-let-7a, forces DNA (7) to release through hybridization of inputs to the substrate, followed by the formation of duplex DNA (7)/ADD-II. This inhibits the activation of CRA, leading to a false output. Thus, the NAND logic produces the inverted result of the AND gate. All of the CL output signals are properly observed in accord with the NAND gate operation, in which a true output of 1 is generated for all combinations of binary inputs except for (1, 1) input situation that give a false output of 0 (Fig. S5).

6.5. IMPLICATION gate

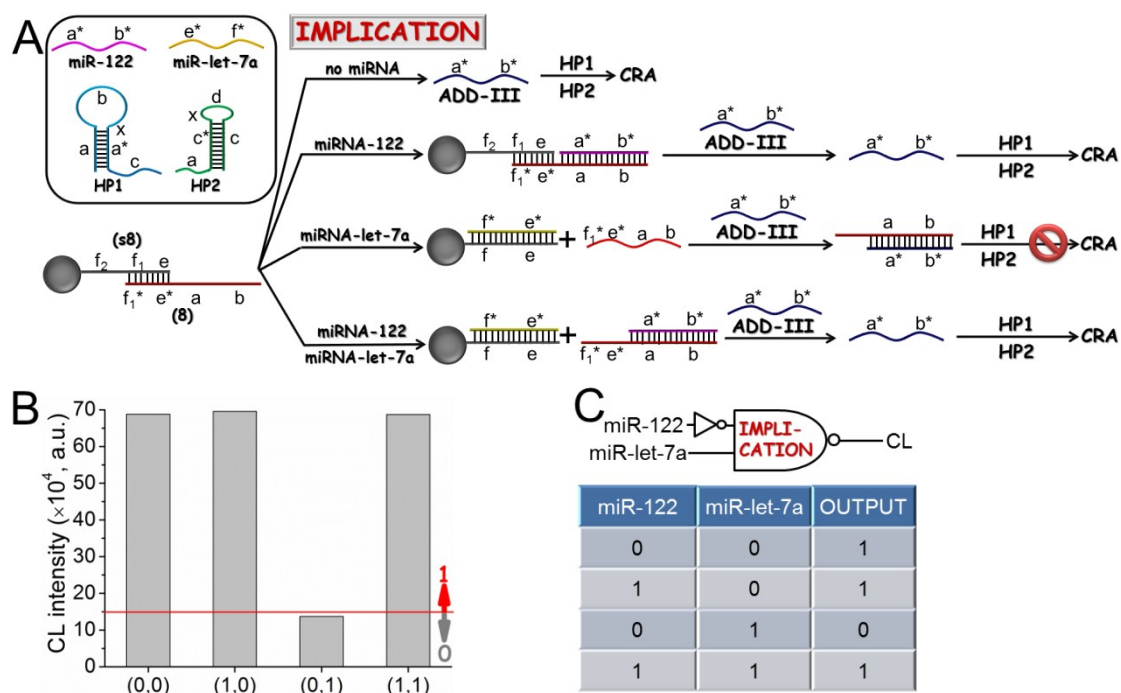


Fig. S7 (A) Diagrammatic representation, (B) CL results, and (C) truth table of IMPLICATION

logic gate that is activated by miR-122 and miR-let-7a as inputs and connected to CRA reaction to produce CL outputs.

Likewise, an IMPLICATION logic gate is built (Scheme 3D). In the absence of any input, ADD-III can activate the CRA to produce a CL signal (true input of 1). Upon the addition of input miR-let-7a that is complementary to substrate (s8), DNA (8) is dissociated from the substrate, promoting the formation of duplex DNA (8)/ADD-III and forcing the CRA to stop. On the other hand, as long as input miR-122 is applied into the system, such as the input state (1, 0) and (1, 1), since miR-122 is complementary to the overhang of DNA (8), the ADD-III are free to initiate the CRA. Thus, IMPLICATION gate gives an output of 0 only when input miR-let-7a is present without the other input, which generates the inverted results of INHIBIT gate (Fig. S6).

References

- 1 H. Dong, K. Hao, Y. Tian, S. Jin, H. Lu, S.-F. Zhou and X. Zhang, *Biosens. Bioelectron.*, 2014, **53**, 377-383.
- 2 H. Dong, X. Meng, W. Dai, Y. Dai, H. Lu, S. Zhou and X. Zhang, *Anal. Chem.*, 2015, **87**, 4334-4340.
- 3 Z. Yuan, Y. Zhou, S. Gao, Y. Cheng and Z. Li, *ACS Appl. Mater. Interfaces*, 2014, **6**, 6181-6185.
- 4 Q. Wang, R.-D. Li, B.-C. Yin and B.-C. Ye, *Analyst*, 2015, **140**, 6306-6312.
- 5 X. Li, D. Li, W. Zhou, Y. Chai, R. Yuan and Y. Xiang, *Chem. Commun.*, 2015, **51**, 11084-11087.
- 6 X. Guo, X. Yang, P. Liu, K. Wang, Q. Wang, Q. Guo, J. Huang, W. Li, F. Xu and C. Song, *Analyst*, 2015, **140**, 4291-4297.
- 7 Z. Jiang, H. Wang, X. Zhang, C. Liu and Z. Li, *Anal. Methods*, 2014, **6**, 9477-9482.
- 8 N. Hao, X.-L. Li, H.-R. Zhang, J.-J. Xu and H.-Y. Chen, *Chem. Commun.*, 2014, **50**, 14828-14830.
- 9 L. Cui, X. Lin, N. Lin, Y. Song, Z. Zhu, X. Chen and C. J. Yang, *Chem. Commun.*, 2012, **48**, 194-196.
- 10 L. Cui, Z. Zhu, N. Lin, H. Zhang, Z. Guan and C. J. Yang, *Chem. Commun.*, 2014, **50**, 1576-1578.